

SUPPORTING INFORMATION

Bi-layer lithium phosphorous oxynitride/aluminium substituted lithium lanthanum titanate as promising solid electrolyte for long-life rechargeable lithium-oxygen batteries

Hang T.T. Le, Ramchandra S. Kalubarme, Duc Tung Ngo, Harsharaj S. Jadhav, and Chan-Jin Park*

Department of Materials Science and Engineering, Chonnam National University, 77,
Yongbongro Bukgu Gwangju 500-757, South Korea

* Corresponding author.

Tel.: Tel: +82-62-530-1704;

Fax: +82-62-530-1699

E-mail address: parkcj@jnu.ac.kr

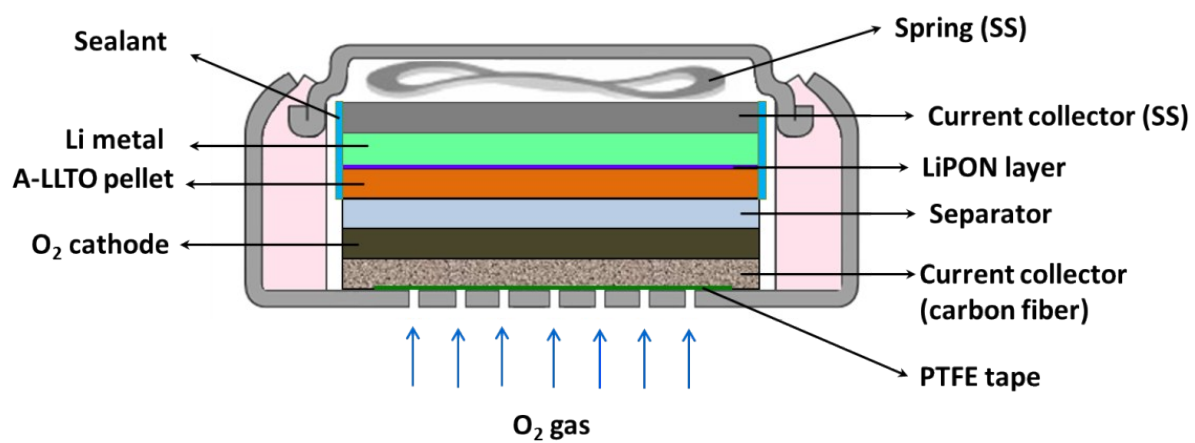


Fig. S1 Configuration of the modified coin-type Li-O₂ cell employing LiPON/A-LLTO solid electrolyte.

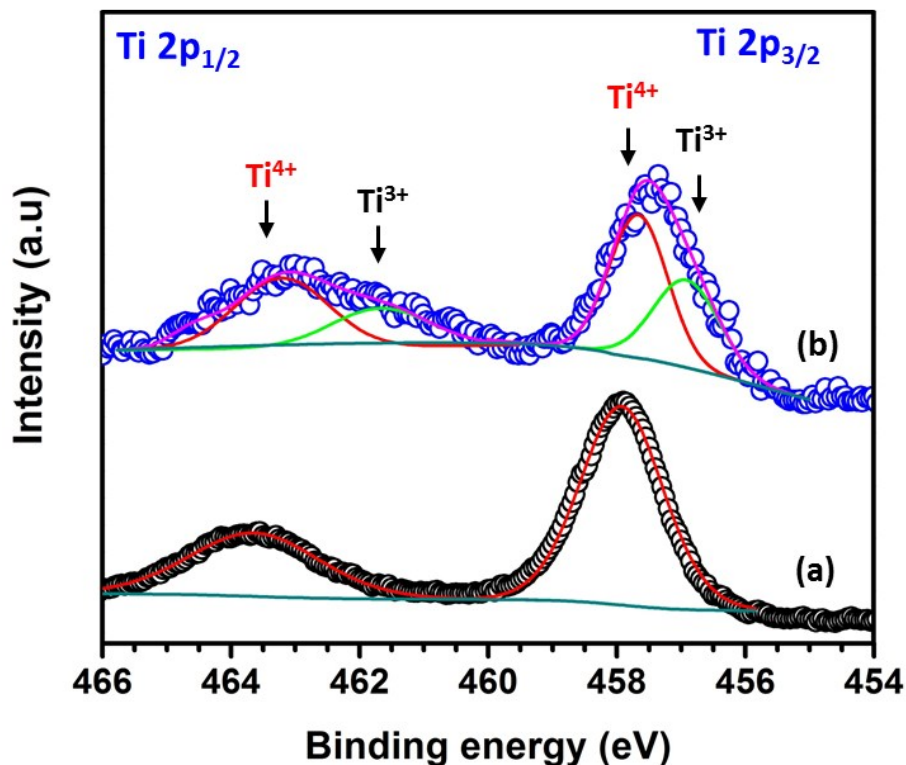


Fig. S2 Ti 2p spectra for A-LLTO ceramics (a) before and (b) after contact with Li metal after 120 h.

Typical Ti 2p photoelectron spectra are shown in **Fig. S3**. For the pristine A-LLTO sample, doublet peaks were detected at 463.7 eV for Ti 2p_{1/2} and 458.0 eV for Ti 2p_{3/2}, as shown in **Fig. S2a**. The separation between the Ti 2p_{1/2} peak and Ti 2p_{3/2} peak was 5.7 eV and the area ratio was close to 2:1. This is in good agreement with the oxidation state of Ti⁴⁺ coordinated with six O²⁻ ions in TiO₂, as reported in other studies.^{1, 2} After direct contact with the Li metal electrode for 120 h, the location of the peaks shifted to 463.1 eV for Ti 2p_{1/2} and 457.5 eV for Ti 2p_{3/2} as shown in **Fig. S2b**. The deconvolution of the Ti 2p spectrum clearly showed the presence of a Ti-suboxide state, namely Ti³⁺, which has been similarly found in the literature.^{1, 3, 4} This is indicative of the reduction of Ti⁴⁺ into Ti³⁺ after A-LLTO made contact with the metallic Li electrode.

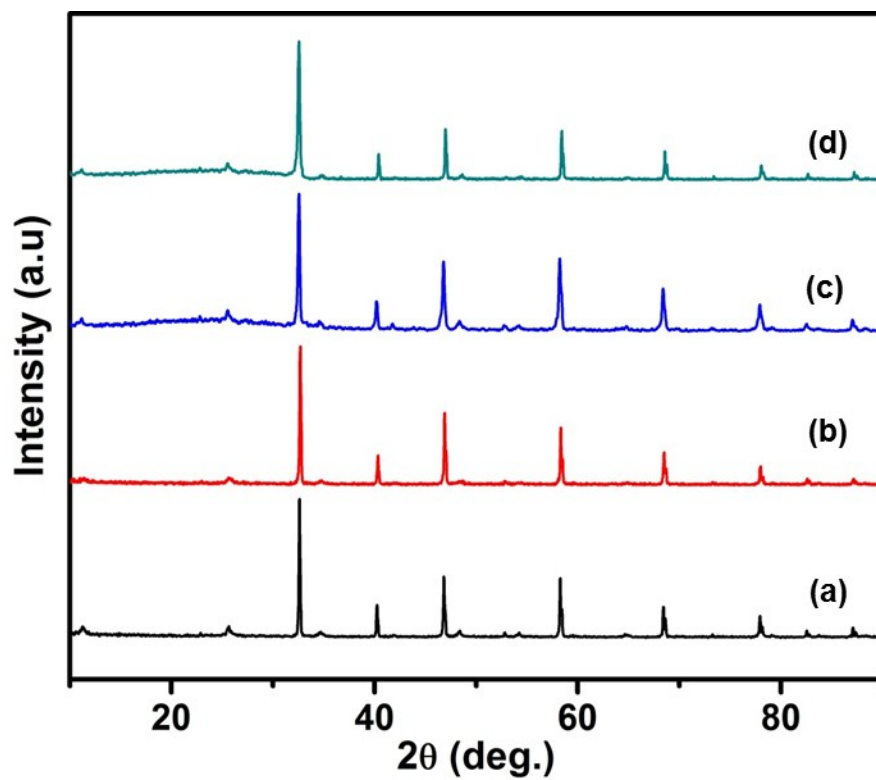


Fig. S3 XRD patterns for A-LLTO and LiPON/A-LLTO/LiPON pellet before and after contact with metallic Li electrode for 120 h: (a) before contact (A-LLTO), (b) after contact (A-LLT), (c) before contact (LiPON/A-LLTO/LiPON), and (d) after contact (LiPON/A-LLTO/LiPON).

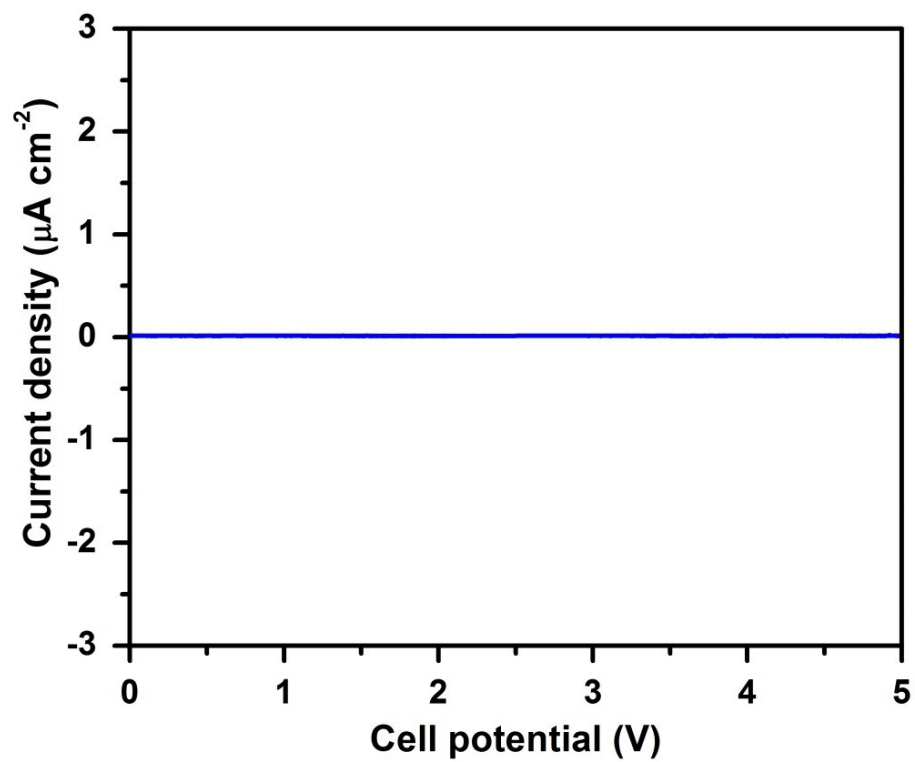


Fig. S4 Linear voltammogram for Ag/Pt/LiPON/A-LLTO/LiPON/Pt/Ag in the potential range of 0 to 5 V.

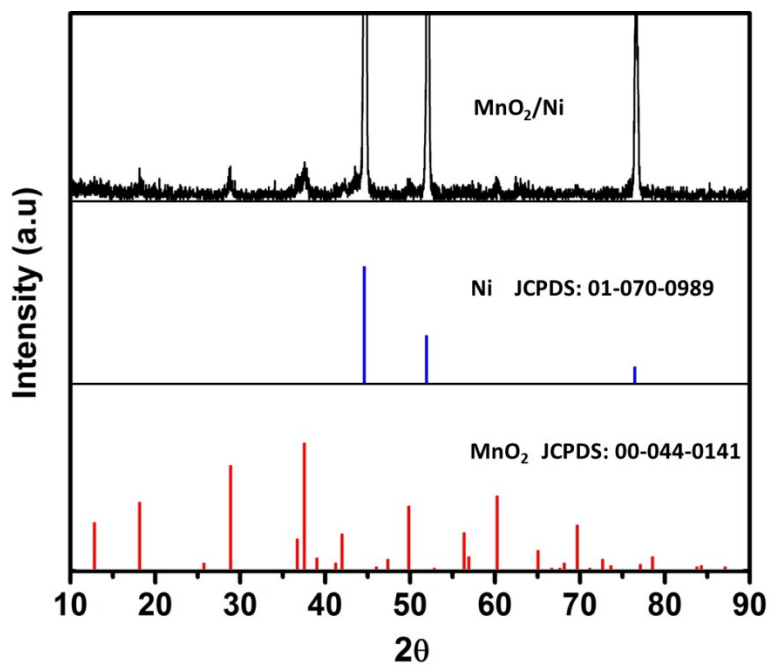


Fig. S5 XRD patterns of MnO_2 nanosheet arrays supported on Ni foam after annealing at 450°C for 5 h.

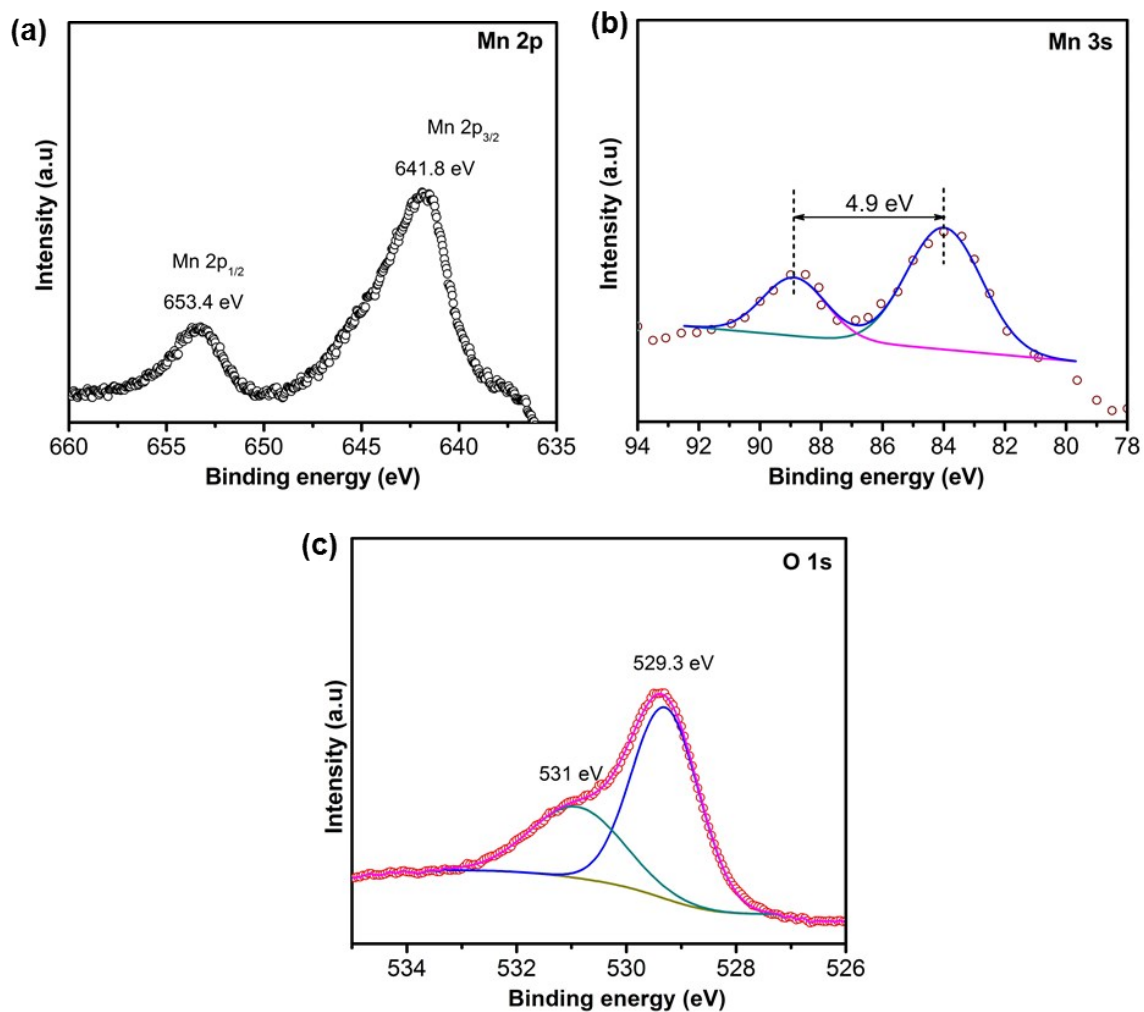


Fig. S6 XPS spectra corresponding to (a) Mn 2p, (b) Mn 3s, and (c) O 1s regions for the obtained MnO₂ NS arrays supported on Ni foam.

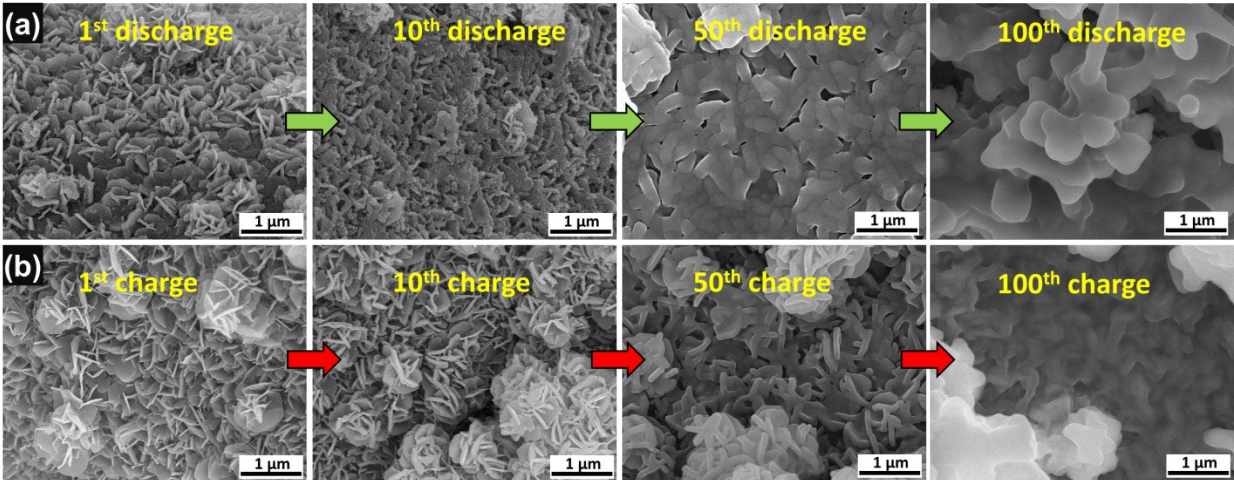


Fig. S7 Morphological change of MnO₂ based oxygen electrode detached from the Li-O₂ cell using Li metal electrode protected by LiPON/A-LLTO after (a) discharge process and (b) charge process at a limited capacity mode of 1000 mA h g⁻¹.

Fig. S7 shows the morphological change after different discharge-charge cycles of the MnO₂ electrode in Li-O₂ cell with LiPON/A-LLTO under constant capacity mode (1000 mA h g⁻¹). As can be clearly observed, after the discharge process, the surface of the MnO₂ electrode was almost totally covered with reaction products, especially for a long duration of cycling such as 50 and 100 cycles. This reveals the amount of the products was formed increasingly according to the cycle number of discharge-charge. After the charge process, only when there were less than 10 cycles, the morphology of the MnO₂ electrode maintained the integrity of the pristine electrode as seen in **Fig. 5**. From the 10th cycle on (for example at the 50th and 100th cycles), after the charge process the electrode surface was still covered with a thick layer of reaction products, demonstrating the decreasing catalysis of the MnO₂ material.

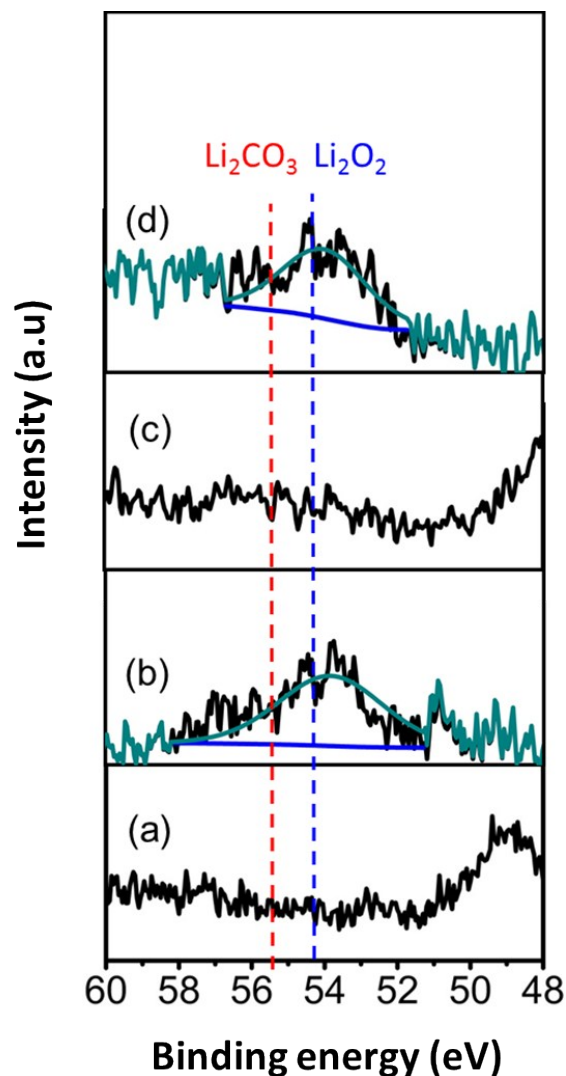


Fig. S8 XPS spectra for Li 1s on MnO₂ based oxygen electrode detached from the Li-O₂ cell using Li metal electrode protected by LiPON/A-LLTO, (a) pristine (b) after 10th discharge, after (c) after 10th charge, and (d) after 100th charge.

As seen in **Fig. S8b**, the typical peak of the Li₂O₂ reaction product was detected after discharging of the 10th cycle. However, immediately after the 10th charge, the peak disappeared, similar to the pristine electrode, suggesting the catalysis of the MnO₂ material in the Li-O₂ cell. Unfortunately, the peak of Li₂O₂ remained even after the charge process at the 100th cycle. This indicates the catalysis degradation of MnO₂ electrode, which is consistent with the SEM results in **Fig. S7**.

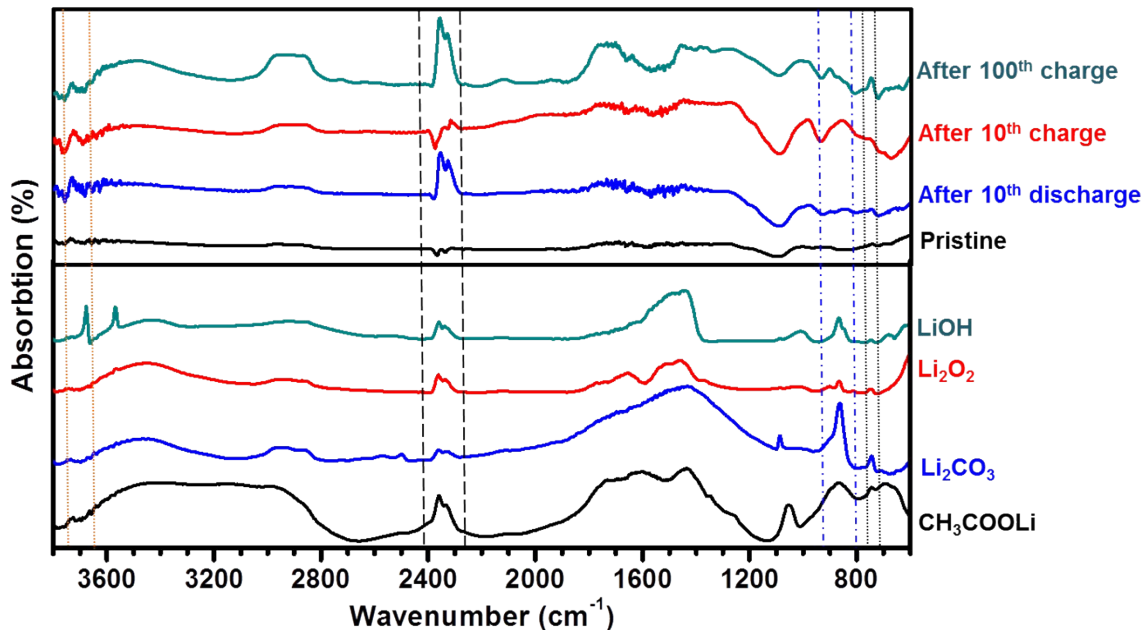


Fig. S9 FTIR spectra of MnO₂ based oxygen electrode detached from the Li-O₂ cell using a Li metal electrode protected by LiPON/A-LLTO in comparison with the reference compounds, which are generally considered as products formed during cycling process.

To further confirm the presence of the reaction products, the FTIR spectra of the MnO₂ electrode after several ten discharge-charge cycles were analysed. For comparison, some reference compounds such as LiOH, Li₂O₂, Li₂CO₃, and CH₃COOLi were also analysed. Obviously, for pristine MnO₂ electrode, no typical peak was found in FTIR spectrum. After 10 cycles of discharge, a doublet peak was detected at the wavenumber range from 2260 to 2400 cm⁻¹, suggesting the presence of Li₂O₂ reaction product formed during the discharge process of Li-O₂ cell. Surprisingly, upon subsequent charge process, in particular after 10 cycles of charge this doublet peak disappeared absolutely. This illustrates that Li₂O₂ reversible reaction product had been converted completely to the other correspondent species. Thus, in the 10th cycle MnO₂ still showed good catalysis activity. However, after 100 cycles, even in charge state, the doublet peak at the range of 2260 to 2400 cm⁻¹ was still observed in FTIR spectrum of MnO₂ electrode, even with increased intensity. The presence of this peak can be assigned to the presence of remained Li₂O₂ (which was confirmed by XPS spectrum in shown **Fig. S8d**) as well as the products of electrolyte decomposition such as LiOH, Li₂CO₃, and CH₃COOLi.⁵⁻⁸ During cycling the electrolyte decomposition products would be accumulated continuously and cover entire the

surface of MnO_2 (**Fig. S7**). Simultaneously, the electrolyte decomposition products would hinder the transportation of the superoxide species, electrons and lithium ions within the cathode during subsequent cycling.⁸ Consequently, the deterioration of the cathode led to the failure of the Li-O_2 cell in spite of using Li metal electrode protected by LiPON/A-LLTO.

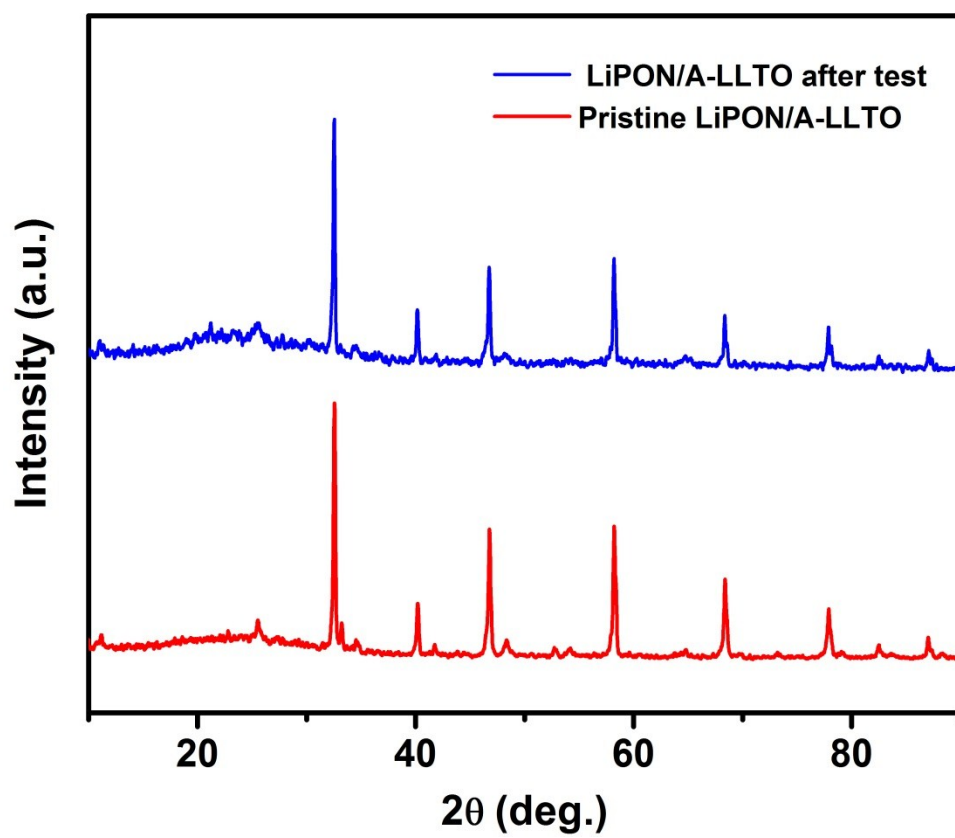


Fig. S10. XRD patterns of the pristine LiPON/A-LLTO and LiPON/A-LLTO after the test for 129 cycles under the limited capacity mode of 1000 mA h g^{-1} .

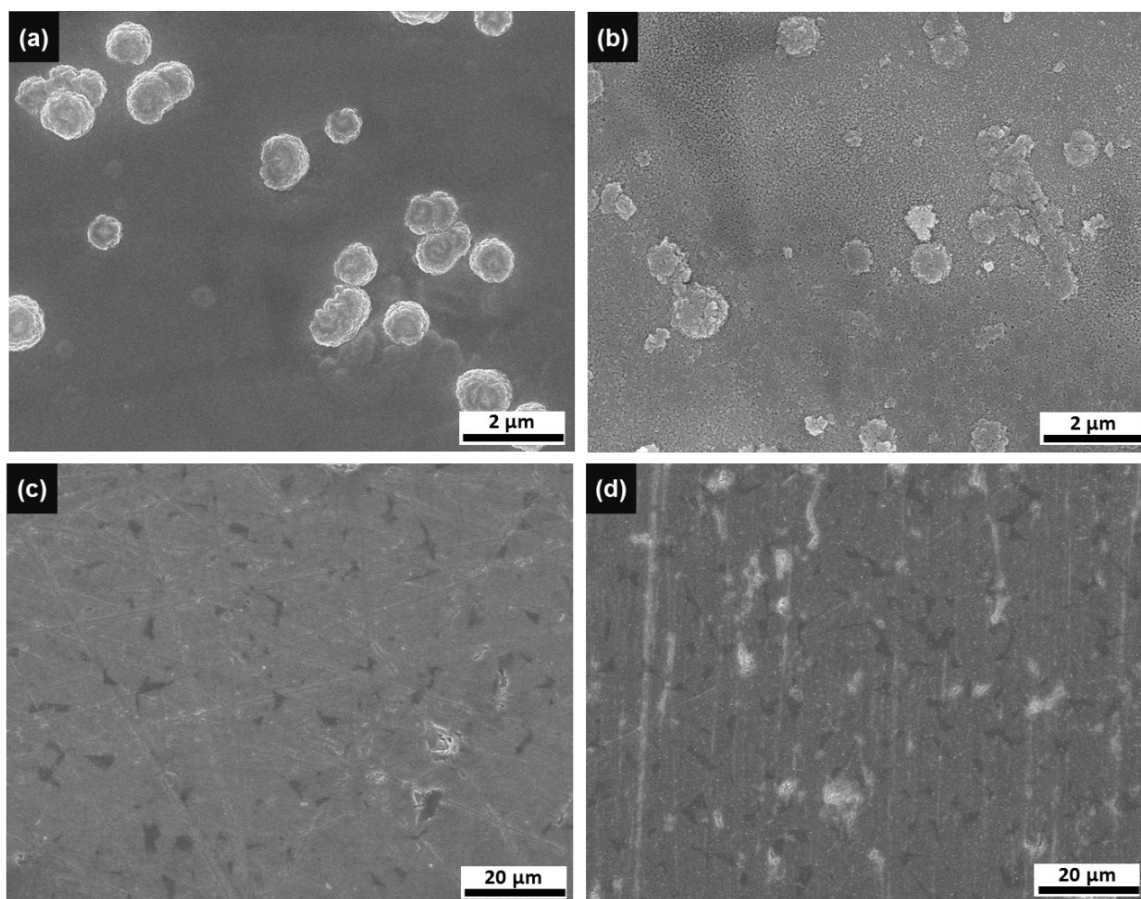


Fig. S11 SEM images of the surface of LiPON and A-LLTO. (a) and (b) correspond to LiPON before and after the test for 129 cycles, respectively, and (c) and (d) correspond to A-LLTO before and after test under the limited capacity mode of 1000 mA h g^{-1} , respectively.

References

1. Q. N. Pham, C. Bohnke and O. Bohnke, *Surf. Sci.*, 2004, **572**, 375-384.
2. C.-L. Li, B. Zhang and Z.-W. Fu, *Thin Solid Films*, 2006, **515**, 1886-1892.
3. D.-Y. Lu, M. Sugano, X.-Y. Sun and W.-H. Su, *Appl. Surf. Sci.*, 2005, **242**, 318-325.
4. B. D. Mukri, G. Dutta, U. V. Waghmare and M. S. Hegde, *Chem. of Mater.*, 2012, **24**, 4491-4502.
5. Z.-L. Wang, D. Xu, J.-J. Xu and X.-B. Zhang, *Chem. Soc. Rev.*, 2014, **43**, 7746-7786.
6. A. Kraytsberg and Y. Ein-Eli, *J. Power Sources*, 2011, **196**, 886-893.
7. S. A. Freunberger, Y. Chen, N. E. Drewett, L. J. Hardwick, F. Bardé and P. G. Bruce, *Ange. Chem. Int. Ed.*, 2011, **50**, 8609-8613.
8. J.-J. Xu, Z.-L. Wang, D. Xu, L.-L. Zhang and X.-B. Zhang, *Nat. Commun.*, 2013, **4**, 2438.